

SOME MODELS OF THE EMISSION-LINE REGION OF 3C 273*

JOHN N. BAHCALL† AND BEN-ZION KOZLOVSKY

California Institute of Technology, Pasadena, California

Received July 24, 1968

ABSTRACT

Models for the emission-line region of 3C 273 are derived by using ionization distributions calculated with extrapolated forms of the observed photon flux. The calculated ionization distributions, which are different from those assumed by previous workers, are used to make estimates of the relative abundances of H, He, O, Ne, Mg, and Fe. Estimates are also given of the physical parameters that characterize the emission-line region.

I. INTRODUCTION

We present models for the emission-line region of 3C 273 that have been derived by using extrapolated forms of the observed photon flux. The models are based on the hypothesis (Schmidt 1963) that the redshifts of quasi-stellar sources are cosmological in origin. Our work differs from that of previous authors (Greenstein and Schmidt 1964; Shklovsky 1965; Osterbrock and Parker 1966; Burbidge *et al.* 1966) in that we calculate, instead of assume, the ionization distribution of the nebula. The emission-line region is required to be optically thin to electron scattering. Our calculated ionization distributions, which turn out to be different from those assumed by the previous workers, enable us to make order-of-magnitude estimates of the relative abundances of H, He, O, Ne, Mg, and Fe. We also derive estimates of the physical parameters that characterize the emission-line region.

In § II we describe the basic assumptions underlying our models, and in § III we outline the calculational methods used to obtain the ionization distributions and line strengths. The principal features of the computed ionization distributions are described in § IV and in Figures 1–5. The calculated line strengths for a typical model are given in Table 2, which is discussed in § V. The observed and calculated line strengths are compared in § VI. This section also contains a discussion of the helium abundance, the characteristic parameters of the emission-line region, and our method of calculating the strengths of the observed Fe II emission lines that are presumably produced by photo-excitation (Wampler and Oke 1967). In § VII we describe the effect of some parameter variations on the predicted line strengths; the photo-ionization cross-sections used in our work are described in the Appendix. In § VIII we mention some of the improvements that are required in our treatment in order to make the calculations fully self-consistent. The principal conclusions from our work are summarized in § IX.

II. DESCRIPTION OF MODELS

Our models, following Greenstein and Schmidt (1964), presume a small central object that emits a strong continuum flux and a large gas cloud that surrounds the central source and emits the observed line radiation. We assume that the continuum intensity in the far ultraviolet emitted by the central source can be obtained from the observed intensity in the visual part of the spectrum by a smooth extrapolation which is not very steep. In particular, we assume that for 3C 273 the central object emits a continuum

* Supported in part by the National Science Foundation under grants GP-7976, GP-9114, and the Office of Naval Research under grant Nonr-220(47).

† Alfred P. Sloan Foundation Fellow.

flux $F_\nu d\nu$, in ergs per second, that has the form

$$F_\nu = F_0, \quad \lambda > 912 \text{ \AA}, \quad (1a)$$

$$F_\nu = F_0 \left(\frac{\lambda}{912} \right)^{+\alpha}, \quad \lambda < 912 \text{ \AA}. \quad (1b)$$

For our standard models we took F_0 from the photoelectric observations of Oke (1965), i.e., $F_0 = 8 \times 10^{+30}$ ergs sec⁻¹ (cps)⁻¹, and used $\alpha = 0.7$. We describe in § VII the effect of using different assumed values of F_0 and α . We shall see in § VII that the predicted line strengths from the most highly ionized ions, which could produce coronal lines, are extremely sensitive to the assumed form of the continuum flux at high frequencies.

The central, continuum source is assumed to be responsible for the ionization of the large gas cloud and for the short-term variations in the optical radiation (Smith and Hoffleit 1963; Sharov and Efremov 1963, 1964). Since the continuum radiation must be capable, by assumption, of exhibiting short-term variations ($\lesssim 1$ year), the large gas cloud (dimensions \gtrsim several parsecs) surrounding the central source must be optically thin to electron scattering. This requirement already distinguishes our models from those of most previous authors. The gas cloud must therefore be in a thin shell or in filaments distributed throughout the volume. In the models described in this paper, we assume that the material is in the form of filaments or condensations, following Schmidt (1964; cf. also Woltjer 1967). The condensations occupy a fraction ϵ of the total volume of the large gas clouds; each filament has the same temperature, chemical composition, and total density. Our computer program is sufficiently flexible to permit the filling factor ϵ , the temperature, the chemical composition, or the density to depend on the distance from the central source, but we have not found it necessary to adopt such dependences in order to reproduce the established features of the emission-line spectrum of 3C 273.

III. CALCULATIONAL METHOD

The principal quantity we want to calculate is the intensity of each emission line. First, however, we must find, for each element A of interest, the number densities, $N_{A,i}(r)$, in the i th stage of ionization at a distance r from the central source. We must also know the optical depth $\tau_\nu(r)$ at each frequency ν . The radiation flux $\phi_\nu(r)$ (in photons per square centimeter per second), which is responsible for photo-ionization, is, if radiation emitted in the large gas cloud is neglected,

$$\phi_\nu(r) = \frac{F_\nu e^{-\tau_\nu(r)}}{h\nu(4\pi r^2)}. \quad (2)$$

The ratio of the continuum emission produced by hydrogen, helium, and free electrons in the large cloud to that emitted by the central source is (Seaton 1960)

$$\frac{\text{(continuum from large cloud)}}{\text{(continuum from central source)}} \approx \epsilon N_e^2 \gamma h V / F_\nu, \quad (3a)$$

$$\lesssim 0.01, \quad (3b)$$

where N_e is the electron density, h is Planck's constant, V is the total volume, and γ is a quantity tabulated by Seaton. The above relation was derived by assuming that there is no absorption by the large gas cloud of the radiation emitted by the central source. This assumption can be justified for wavelengths greater than 912 Å by detailed calculations of the kind described in § IV. For wavelengths shorter than 912 Å, for which absorption is important, we use the "on the spot" approximation for hydrogen and helium, i.e., we assume that emitted photons are reabsorbed after traveling only a

short distance in the outer gas cloud. We have therefore neglected the emission by hydrogen and helium in the large cloud. We have also neglected emission by heavy elements in the gas cloud (cf., however, § VIII).

We now summarize the basic equations we have used.

We assume a steady-state balance between ionization from ground states and recombination from the continuum. This balance implies that

$$N_{i+1}(r) \sum_k \alpha^k_{i+1} = N_i \left[\int_0^\infty \phi_\nu(r) \sigma_i(\nu) d\nu + \langle \sigma v \rangle_i \right]. \quad (4)$$

Here α^k is the recombination coefficient to the level k , $\sigma(\nu)$ is the photo-ionization cross-section (which is, of course, zero for frequencies less than the ionization frequency), and $\langle \sigma v \rangle$ is the rate of ionization by electron collisions. For simplicity we have suppressed everywhere the element label A ; we follow this practice in what follows wherever it is convenient and clear. The optical depth $\tau_\nu(r)$ was calculated from the relation

$$\tau_\nu(r) = \epsilon \int_0^r dr' [\sigma_{\nu, \text{H I}} N^{\text{H I}}(r') + \sigma_{\nu, \text{He I}} N^{\text{He I}}(r') + \sigma_{\nu, \text{He II}} N^{\text{He II}}(r')]. \quad (5)$$

The factor ϵ occurs because of our assumption that the emitting material is in the form of filaments. It is convenient for computational purposes to define a quantity $Y_{A,i}(r)$ by the equation

$$Y_{A,i}(r) = N_{A,i+1}(r) / N_{A,i}(r). \quad (6a)$$

We can calculate $Y_{A,i}(r)$ directly from equation (4). The quantity $N_{A,i+1}(r)$ is given by

$$N_{i+1}(r) = N_1(r) \prod_{k=1}^i Y_k, \quad (6b)$$

where

$$\prod_{k=1}^i Y_k \equiv Y_1 Y_2 \dots Y_i.$$

Let $S_{A,i}(r)$ be the fraction of the element A that is in the ionization stage i . Then

$$S_1(r) = \left[1 + \sum_{i=1}^c \left(\prod_{m=1}^i Y_m \right) \right]^{-1}, \quad (7a)$$

$$S_{i+1}(r) = \left(\prod_{k=1}^i Y_k \right) / \left(1 + \sum_{l=1}^c \prod_{m=1}^l Y_m \right), \quad i \geq 1, \quad (7b)$$

and

$$\sum_{i=1}^{c+1} S_i(r) \equiv 1. \quad (7c)$$

Here $c + 1$ is the total number of stages of ionization for the element A .

In carrying out the numerical calculations, we first determine the hydrogen and helium ratios by number, i.e., the Y 's. At an initial point r_1 (< 1 pc), we assumed that all the hydrogen was in the stage H I and all the helium was in the stage He III. We then chose a value of the total number density N_{total} and a hydrogen-to-helium ratio by number (cf. Table 1). The following relations are satisfied by definition at $r = r_1$:

$$\begin{aligned} N_e(r_1) &= N_{\text{total}}(r_1) \\ &= N^{\text{H I}}(r_1) + 2N^{\text{He III}}(r_1), \end{aligned} \quad (8a)$$

where N_e is the electron number density, and

$$\begin{aligned} N^{\text{H I}}(r_1) &= N^{\text{He I}}(r_1) \\ &= N^{\text{He II}}(r_1) \\ &= 0. \end{aligned} \quad (8b)$$

Equations (4)–(6) can now be solved at a larger radius $r_1 + dr$, for all the hydrogen and helium V 's, N_e , and τ_ν . The results are used to determine these quantities at a still larger radius, etc. The values of $\tau_\nu(r)$ determined in this way are used afterward to determine the heavy-element ratios, or V 's.

TABLE 1
ABUNDANCES BY NUMBER RELATIVE TO HYDROGEN
ASSUMED IN OUR CALCULATIONS OF
EMISSION-LINE STRENGTHS

Element	Relative Abundance
He	$7 \times 10^{-2}, 7 \times 10^{-3}, 7 \times 10^{-4}$
C	2×10^{-4}
N	6×10^{-5}
O	6×10^{-4}
Ne	1×10^{-4}
Na	2×10^{-6}
Mg	4×10^{-5}
Si	3×10^{-5}
Ar	2×10^{-6}
Fe	6×10^{-5}

The emission-line strengths can be calculated from the dimensionless integrals:

$$I_{A,i} = \int DS_{A,i}(r') \frac{N_e(r')}{(10^{+6} \text{ cm}^{-3})} \frac{dV'}{(1 \text{ pc})^3}, \quad (9a)$$

where D is a suppression factor that takes account of electron de-excitation as well as photon decays other than the ones in which we are interested. For a transition of interest from a state r to a state s in which a set of alternate final states $\{t\}$ exists,

$$D = A_{r \rightarrow s} / \left(\sum_t A_{r \rightarrow t} + \langle \sigma v \rangle N_e \right). \quad (9b)$$

The power emitted in a line of wavelength λ formed by recombination is

$$\begin{aligned} E_{A,i}(\text{recombination}) &= 5.8 \times 10^{+42} \text{ ergs sec}^{-1} \epsilon I_{A,i+1} \left(\frac{N_{\text{element}}}{10^{+6} \text{ cm}^{-3}} \right) \\ &\times \left(\frac{10^{+3} \text{ \AA}}{\lambda} \right) \left(\frac{a}{10^{-14} \text{ cm}^3 \text{ sec}^{-1}} \right). \end{aligned} \quad (10)$$

The corresponding equation for a line formed by electron excitation is

$$\begin{aligned} E_{A,i}(\text{electron excitation}) &= 5.0 \times 10^{+49} \text{ ergs sec}^{-1} \epsilon I_{A,i} \left(\frac{N_{\text{element}}}{10^{+6} \text{ cm}^{-3}} \right) \left(\frac{10^{+3} \text{ \AA}}{\lambda} \right) \\ &\times \left[\left(\frac{\Omega}{\omega_{\text{initial state}}} \right) T_4^{-1/2} \exp - \left(\frac{\Delta E}{0.861 T_4} \right) \right]. \end{aligned} \quad (11)$$

In equation (11), $\Omega/\omega_{\text{initial state}}$ is the usual collision strength (Seaton 1958), T_4 is the temperature in 10^4 °K, and ΔE is the excitation energy in electron volts. For the conditions defined by our problem, excitations by protons and hydrogen atoms are negligible (cf. Bahcall and Wolf 1968). The equivalent width, w , of an emission line that emits an amount of power E in a line of wavelength λ is:

$$w = 0.42(\lambda/10^3 \text{ \AA})^2 \left(\frac{E}{10^{43} \text{ ergs sec}^{-1}} \right) \left(\frac{8 \times 10^{30} \text{ ergs sec}^{-1} (\text{cps})^{-1}}{F_\nu} \right). \quad (12)$$

IV. DEPENDENCE OF IONIZATION STAGES ON DISTANCE FROM CENTRAL SOURCE

We report in this section the ionization distribution in some models of 3C 273 that have the following parameters: $\epsilon = 10^{-3}$, $N_e(r=0) = 2 \times 10^{16} \text{ cm}^{-3}$, and electron temperature $T = 1.7 \times 10^4$ °K. Some discussion of the effects of varying these parameters is given in § VIc. The abundances by number used in our calculations are given in Table 1. With only two exceptions, the values used are the usual *solar* abundances taken from Zirin (1966). The two exceptions are the sodium abundance, which is taken equal to the average cosmic abundance given by Allen (1963), and the helium abundance. We have tried three different values for the helium abundance, 7×10^{-2} , 7×10^{-3} , and 7×10^{-4} , because the opacity of helium influences the predicted line strengths of other elements and because the observed line strengths suggest (cf. § VI) that the correct helium abundance is less than the solar value of 5.5×10^{-2} (Bahcall, Bahcall, and Shaviv 1968).

We show in Figures 1–5 the variation with r of the fractional abundances of the various ionization stages of H, He, C, Mg, and Fe. The largest radius considered is 15 pc, which corresponds approximately (cf. § V) to the outer radius of the large gas cloud in our standard model. Figures 1 and 2 show the dependence of H I, He I, He II, and N_e on r for $(\text{He}/\text{H}) = 7 \times 10^{-2}$ and 7×10^{-3} , respectively.

A few features deserve special comment:

1. The highest stages of ionization in our models dominate over almost the entire range of r (see especially Figs. 3–5); the lower stages of ionization are significantly populated only for radii greater than 10 pc. Note in Figures 3–5 that C III, C IV, Mg II, and Fe II, all of which give rise to important emission lines in quasi-stellar sources, are relatively populous only in the outer edges of the nebula. This situation exists because of the large absolute luminosity of 3C 273 and the flat ultraviolet spectrum we have assumed. Both high stages of ionization (e.g., Fe XI and Fe XIII) and low stages of ionization (e.g., Mg II, Fe II, and O III) are produced by the assumed photon flux. The calculated ionization distribution is reminiscent of the wide range of ionization stages found in Seyfert galaxies (see, e.g., the recent study of NGC 4151 by Oke and Sargent 1968), which may also be caused by predominantly photon ionization with a relatively flat spectrum. The very high stages of ionization of Fe (e.g., Fe XIII and Fe XIV) are characteristic coronal features but are here due to the strong ionizing flux of photons, not high electron temperatures.

2. The ionization distribution we calculate differs significantly from any of the assumed distributions postulated by previous authors. For example, Greenstein and Schmidt (1964) assumed that the ionization distribution in the emission-line region was similar to that in planetary nebulae. Our calculations indicate that, among other things, the higher stages of ionization are much more populated in 3C 273 than in planetary nebulae because of the much larger intrinsic luminosity and flatter spectrum that characterize quasi-stellar sources. Osterbrock and Parker (1966) assumed that the second through sixth ionization stages of the most abundant elements were equally populated and contained all of the ions. This assumption is in serious conflict with our calculated results. Burbidge *et al.* (1966) assigned various ionization stages to the three different

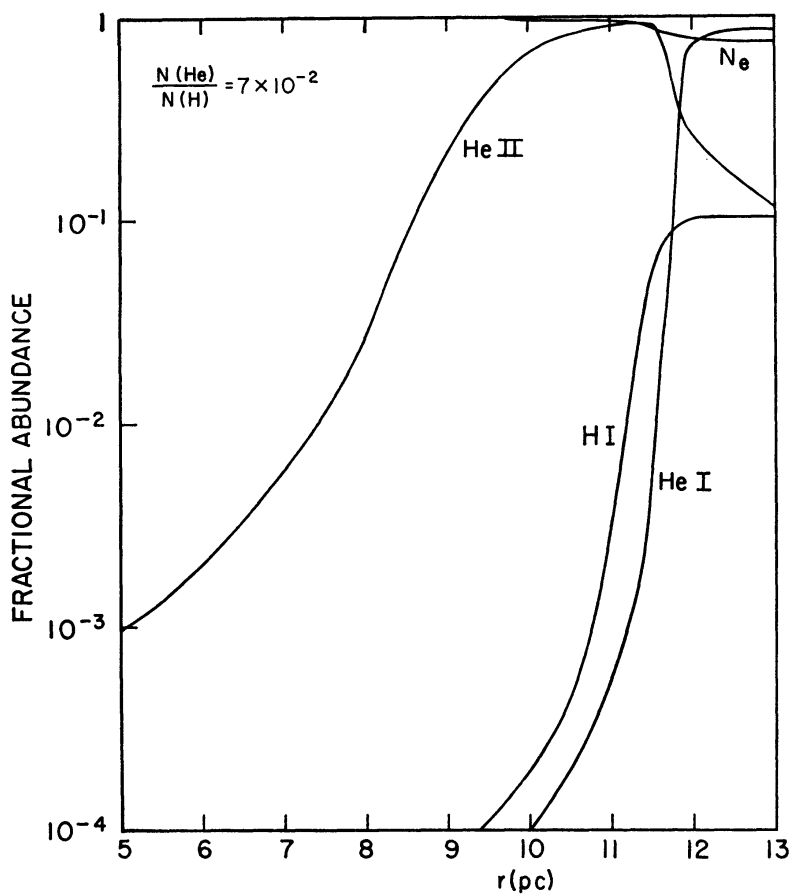


FIG. 1.—Fractional abundance of H I, He I, He II, and N_e (electron density) as a function of distance from the central source for $N(\text{He})/N(\text{H}) = 7 \times 10^{-2}$. Fractional abundance of $N_{A,i}$ is defined as $(N_{A,i}/\sum_j N_{A,j})$.

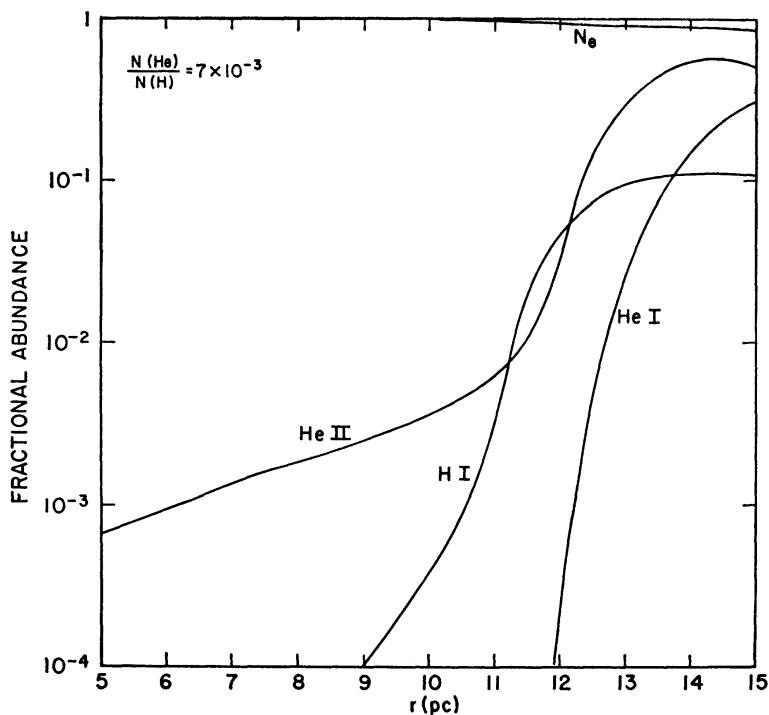


FIG. 2.—Fractional abundance of H I, He I, He II, and N_e , as a function of distance from the central source for $N(\text{He})/N(\text{H}) = 7 \times 10^{-3}$.

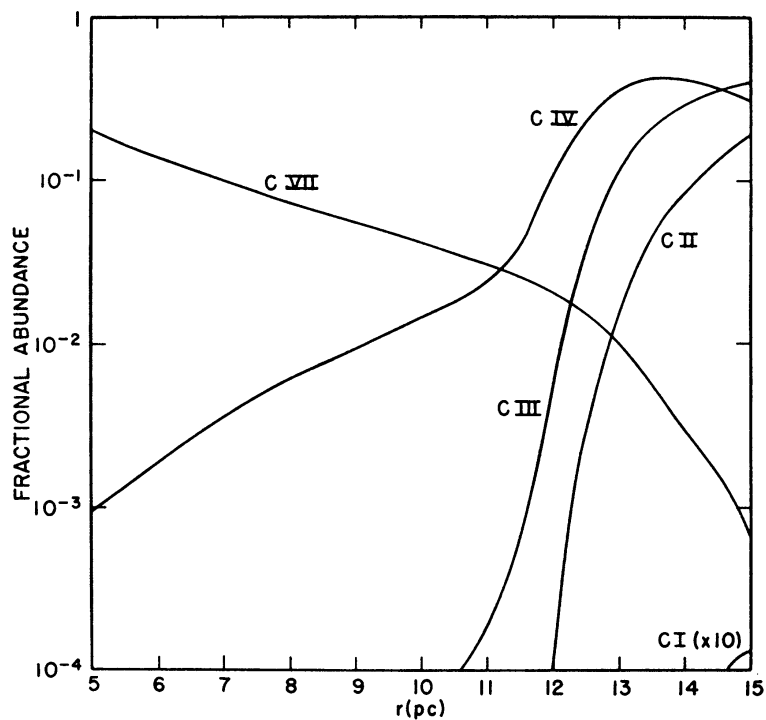


FIG. 3.—Fractional abundance of some carbon ions as a function of distance from the central source. Here $N(\text{He})/N(\text{H}) = 7 \times 10^{-3}$. Notice that C III and C IV, which give rise to important ultraviolet lines, are mainly present in the outer parts of the nebula.

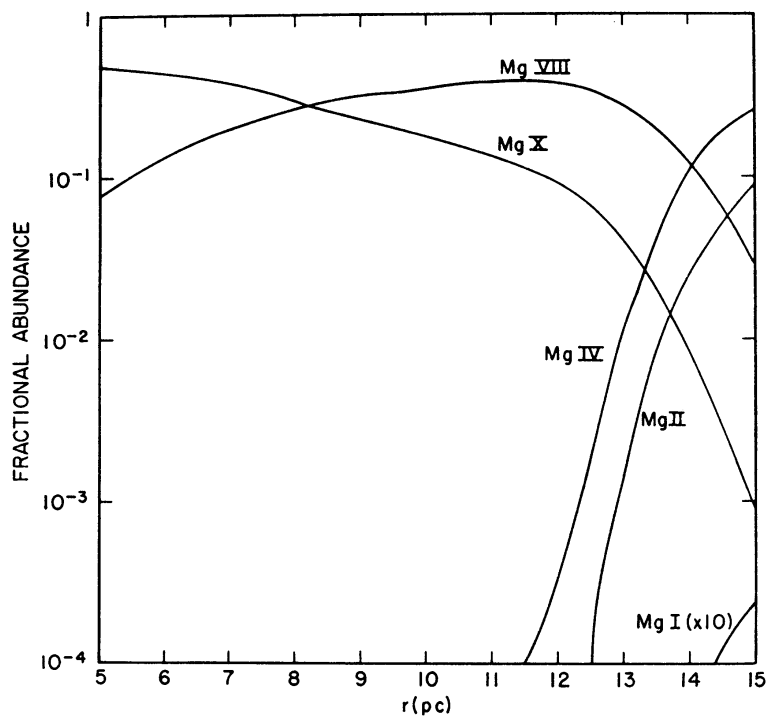


FIG. 4.—Fractional abundance of some Mg ions as a function of distance from the central source. Here $N(\text{He})/N(\text{H}) = 7 \times 10^{-3}$. Notice that Mg II is present only at the outer edge of the nebula.

zones. Their assignments also disagree with our calculated results since, for example, their region containing the easily ionized Mg II is nearest the strong central source.

3. For a helium abundance of 7×10^{-2} (cf. Fig. 1), He II constitutes a significant fraction of the total helium abundance over a large part of the nebular volume. In the corresponding model, He II contributes greatly to the opacity at high frequencies. For a smaller helium abundance, e.g., the value of 7×10^{-3} used to obtain Figure 2, He II begins to build up only at the outer edge of the nebula and therefore contributes a smaller amount to the opacity. This effect on the opacity is of some importance in determining the ionization stages of the other elements.

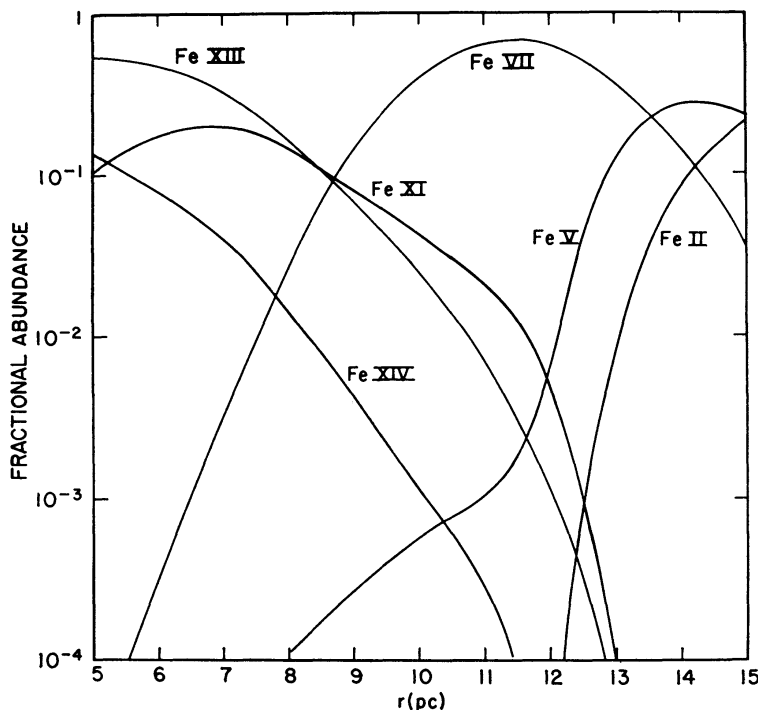


FIG. 5.—Fractional abundance of some Fe ions as a function of distance from the central source. Here $N(\text{He})/N(\text{H}) = 7 \times 10^{-3}$ and $\alpha = 0.7$. Note the presence of very high stages of ionization capable of giving rise to coronal lines.

4. In the outer parts of the nebula, the ratio ($\text{H II}/\text{H I}$) maintains a constant value of about 0.1. This result is due to the dominance of collisional ionization (which is independent of radius) when the central ionizing radiation is greatly reduced. The corresponding effect does not occur for helium because of its high ionization potential. Hence, He I dominates at the outer edge of the nebula.

V. CALCULATION OF EMISSION-LINE STRENGTHS

The outer radius of the emission-line region, R_{em} , was fixed by requiring that the total energy emitted in the Mg II $\lambda 2798$ line be equal to the value of 4×10^{43} ergs sec^{-1} measured by Greenstein and Schmidt (1964). Values of R_{em} equal to 11.4, 14.2, and 14.8 pc were obtained for the models with helium abundances equal to 7×10^{-2} , 7×10^{-3} , and 7×10^{-4} , respectively.

We give in Table 2 the calculated strengths of most of the lines in the observable region of the spectrum of 3C 273 that either appear in Schmidt's (1965) finding list for quasi-stellar sources or have been identified in 3C 273 or other quasi-stellar sources

TABLE 2—Continued

ION	λ_0 (Å) (1)	Ω/ω (2)	E_z (eV) (3)	$\text{He}/\text{H} = 7 \times 10^{-2}$		$\text{He}/\text{H} = 7 \times 10^{-3}$		$\text{He}/\text{H} = 7 \times 10^{-4}$		F_{observed} (10^{+43} ergs sec^{-1}) (10)
				E 10^{+43} ergs sec^{-1} (4)	Eq. W. (Å) (5)	E (10^{+43} ergs sec^{-1}) (6)	Eq. W (Å) (7)	E (10^{+43} ergs sec^{-1}) (8)	Eq. W. (Å) (9)	
Mg II..	2798	10.5	4.42	3	11	3	11	3	11	4GS
	2928	0.1	8.65	2×10^{-3}	6×10^{-3}	2×10^{-3}	6×10^{-3}	2×10^{-3}	6×10^{-3}	
	2930									
Ar IV..	2853.6	0.06	4.43	3×10^{-2}	1×10^{-1}	2×10^{-2}	7×10^{-2}	2×10^{-2}	7×10^{-2}	$< 4 \text{ \AA eq. w.}$
	2868.2									
Ar X...	[5536]	0.01	2.24	1×10^{-3}	2×10^{-2}	1×10^{-3}	2×10^{-2}	1×10^{-3}	2×10^{-2}	
Ar XIV..	[4412]	0.02	2.84	2×10^{-3}	1×10^{-2}	2×10^{-3}	1×10^{-2}	2×10^{-3}	1×10^{-2}	
Fe X...	[6374.5]	0.01	1.94	3×10^{-2}	5×10^{-1}	6×10^{-2}	1	6×10^{-2}	1	
Fe XI..	[7891.9]	0.08	1.57	1	27	1.6	44	1.8	48	
Fe XIII..	[10746.8]	0.3	1.15	3	150	3	160	3	160	
	[10798.0]	0.25	2.3	5×10^{-1}	26	6×10^{-1}	28	6×10^{-1}	28	
Fe XIV	[5302.9]	0.1	2.31	1	13	1	13	1	13	

(Burbidge *et al.* 1966; Wampler and Oke 1967). A few additional lines, such as the He I lines and the coronal lines of Ar and Fe, have been added because of their special interest. The line strengths were calculated by using equations (9)–(11) of § III. The values of $I_{A,i}$ computed for the model with a helium abundance of 7×10^{-3} are given in Table 3. These values of $I_{A,i}$ do not include the suppression factor D defined by equation (9b); this factor was calculated separately for each forbidden line of interest. Note the relatively large values of $I_{A,i}$ for the highest stages of ionization. The strengths and equivalent widths of other lines that might be of special interest to the reader can be easily calculated from equations (10)–(12), Table 3, and Figures 1–5. The recombination coefficients for hydrogen and helium were obtained by interpolation from the work of Seaton (1960). The values of Ω/ω for most of the lines have been taken from the compilations of Osterbrock (1963), Williams (1967), or Bahcall and Wolf (1968), and are given in column 2 of Table 2. The Fe XIII collision strengths were taken from Kurt (1963), and the Fe XIV strength, from Seaton (1964); the collision strengths for the other coronal lines were crudely estimated from the $(m + 1)^2$ rule of Seaton (1964) and could easily be in error by a factor of 3 or more. A few collision strengths were simply guessed from the published values for analogous transitions. The collision strengths listed as (1?) were not estimated, since their exact values were unimportant. The rates of photon decays, i.e., A 's used in calculating the suppression factors (cf. eq. [9b]) for all cases where suppression is significant, were taken from the compilation of Wiese, Smith, and Glennon (1966). The excitation energies of the upper states are denoted by E_x and are given, in electron volts, in column 3 of Table 2.

The computed equivalent widths and total emitted power are given in columns 4–9 of Table 2 for the three models with helium abundances varying from 7×10^{-2} to 7×10^{-4} . The corresponding observed values of the emission strengths are given in the last column; the values determined by Greenstein and Schmidt (1964) are marked by a superscript GS, those measured by Oke (1965) are marked by a superscript O, and those given by Wampler and Oke (1967) are denoted by WO. The upper-limit estimates for the equivalent widths of the unobserved lines are a private communication from Oke (1968).

VI. COMPARISON WITH OBSERVED LINE STRENGTHS

a) General Agreement

The general agreement between the calculated power, using *solar* abundances and $N_{\text{total}} = 2 \times 10^6 \text{ cm}^{-3}$, and the observed strength of the emission lines is satisfactory except for He II $\lambda 4686$ and [O III] 5007. The strongest observed lines, H α , H β , Mg II $\lambda 2798$, and the Fe II lines (cf. § VI*d*), are calculated to have relatively large emission strengths which approximately match the measured values. The many other lines which appear either in the spectra of different quasi-stellar sources or in the finding list of Schmidt (1965) have small calculated strengths. We now examine, in successive subsections, the special problems associated with the helium abundance, the characteristic parameters, the Fe II lines, and the Na I lines.

b) The He Abundance

Oke (1968) has kindly provided us with an upper limit on the equivalent widths for He II $\lambda 4686$ (cf. Table 2). In order to obtain an equivalent width with our models that is as small as Oke's upper limit, we must assume a helium-to-hydrogen number ratio of the order of 5×10^{-3} . (This result is consistent with the findings of Osterbrock and Parker 1966, who, however, assumed a priori a special ionization distribution.) This is a factor of 10 lower than the most recent estimate of the solar helium-to-hydrogen ratio inferred from solar-model calculations (Bahcall *et al.* 1968). The low value of the helium-to-hydrogen ratio required for 3C 273 by the lack of observation of He II $\lambda 4686$ improves

TABLE 3
THE INTEGRALS $I_{A,1}$

STAGE OF IONIZATION	ELEMENT										
	H	He	C	N	O	Ne	Na	Mg	Si	Ar	Fe
I.	$9.3 \times 10^{+2}$	$8.6 \times 10^{+2}$	1.9×10^{-2}	2.5×10^{-1}	9.8×10^{-2}	1.4×10^{-2}	1.3×10^{-4}	1.7×10^{-2}	3.5×10^{-2}	2.0×10^{-1}	2.3×10^{-2}
II.	$2.3 \times 10^{+4}$	$3.7 \times 10^{+3}$	$3.7 \times 10^{+2}$	$1.6 \times 10^{+2}$	$7.0 \times 10^{+1}$	5.5	6.0	$6.5 \times 10^{+1}$	$1.9 \times 10^{+2}$	$1.6 \times 10^{+2}$	$2.5 \times 10^{+2}$
III.		$1.9 \times 10^{+4}$	$1.7 \times 10^{+3}$	$1.5 \times 10^{+3}$	$1.0 \times 10^{+3}$	$1.2 \times 10^{+2}$	$1.6 \times 10^{+2}$	$5.0 \times 10^{+1}$	$4.4 \times 10^{+2}$	$1.0 \times 10^{+3}$	$1.5 \times 10^{+2}$
IV.			$3.9 \times 10^{+3}$	$1.9 \times 10^{+3}$	$3.3 \times 10^{+3}$	$7.7 \times 10^{+2}$	$8.6 \times 10^{+2}$	$4.6 \times 10^{+2}$	$9.6 \times 10^{+2}$	$1.2 \times 10^{+3}$	$8.9 \times 10^{+2}$
V.			$7.3 \times 10^{+3}$	$4.7 \times 10^{+3}$	$1.4 \times 10^{+3}$	$1.9 \times 10^{+3}$	$7.3 \times 10^{+2}$	$1.2 \times 10^{+3}$	$8.8 \times 10^{+2}$	$3.4 \times 10^{+3}$	$1.7 \times 10^{+3}$
VI.			$1.1 \times 10^{+4}$	$1.1 \times 10^{+4}$	$5.1 \times 10^{+3}$	$2.1 \times 10^{+3}$	$9.7 \times 10^{+2}$	$2.3 \times 10^{+3}$	$3.8 \times 10^{+3}$	$2.9 \times 10^{+3}$	$3.3 \times 10^{+3}$
VII.			$1.2 \times 10^{+3}$	$6.3 \times 10^{+3}$	$1.2 \times 10^{+4}$	$4.4 \times 10^{+3}$	$2.1 \times 10^{+3}$	$4.8 \times 10^{+3}$	$5.8 \times 10^{+3}$	$6.5 \times 10^{+3}$	$1.1 \times 10^{+4}$
VIII.				$3.3 \times 10^{+2}$	$2.7 \times 10^{+3}$	$8.9 \times 10^{+3}$	$7.8 \times 10^{+3}$	$7.0 \times 10^{+3}$	$2.8 \times 10^{+3}$	$8.6 \times 10^{+3}$	$3.1 \times 10^{+3}$
IX.					$7.7 \times 10^{+1}$	$6.7 \times 10^{+3}$	$9.3 \times 10^{+3}$	$4.4 \times 10^{+3}$	$2.8 \times 10^{+3}$	$6.1 \times 10^{+2}$	$4.2 \times 10^{+1}$
X.						$5.9 \times 10^{+2}$	$3.3 \times 10^{+3}$	$4.0 \times 10^{+3}$	$2.6 \times 10^{+3}$	$3.4 \times 10^{+2}$	$3.3 \times 10^{+2}$
XI.						9.3	$2.2 \times 10^{+2}$	$1.2 \times 10^{+3}$	$3.3 \times 10^{+3}$	$2.6 \times 10^{+2}$	$1.1 \times 10^{+3}$
XII.							4.6	$8.2 \times 10^{+1}$	$1.7 \times 10^{+3}$	$9.0 \times 10^{+1}$	$1.0 \times 10^{+3}$
XIII.										$1.0 \times 10^{+2}$	$1.7 \times 10^{+3}$
XIV.										$1.7 \times 10^{+2}$	$6.5 \times 10^{+2}$

NOTE.—Here the ratio of the number density of He to that of H is equal to 7×10^{-3} . The radius of the emitting region is 14.2 pc.

somewhat the agreement between the predicted and observed (Schmidt 1968) strength of [Ne III] $\lambda 3869$.¹ The effect of parameter variations on the predicted line strengths of He II is shown in § VII to be only of the order of a factor of 2 or 3. The discrepancy of a factor of 2 between the observed and predicted values of the Balmer lines is consistent with our uncertainties in calculation. It would be useful to attempt a more accurate search for He II $\lambda 4686$.

c) Characteristic Parameters

The identification of Fe II lines in the spectrum of 3C 273 by Wampler and Oke (1967) has led to the recognition that the strengths originally estimated for [O III] $\lambda 5007$ (Greenstein and Schmidt 1964; Oke 1965) are largely due to Fe II. Oke (1968) has kindly

TABLE 4
SOME EMISSION-LINE STRENGTHS AND OTHER QUANTITIES FOR MODELS
WITH DIFFERENT TOTAL DENSITIES

N_{total} (cm^{-3})	R (parsecs)	Mass (M_{\odot})	H β $\lambda 4861$ (\AA)	He II $\lambda 4686$ (\AA)	[O II] $\lambda 3727$ (\AA)	[O III] $\lambda 5007$ (\AA)	[Ne III] $\lambda 3869$ (\AA)	[Ne V] $\lambda 3426$ (\AA)	Telectron scattering
(a) $\epsilon = 10^{-3}$									
6×10^7	1 7	6×10^4	180	9	6×10^{-2}	4	5×10^{-1}	6	2×10^{-1}
2×10^7	3 5	8×10^4	160	8	2×10^{-2}	10	1	8	1.5×10^{-1}
1×10^7	5	1×10^5	140	7	4×10^{-2}	30	2	10	1×10^{-1}
6×10^6	7	2×10^5	120	6	7×10^{-2}	45	2	10	8×10^{-2}
2×10^6	14	6×10^5	105	6	2×10^{-2}	65	2	10	6×10^{-2}
5×10^5	35	2×10^6	95	5	6×10^{-2}	160	2	11	4×10^{-2}
2.5×10^5	55	4×10^6	90	5	8×10^{-2}	170	2	11	3×10^{-2}
(b) $\epsilon = 10^{-4}$									
2×10^7	6 5	6×10^4	120	6	2×10^{-2}	15	2	14	2.5×10^{-2}
2×10^6	29	5×10^5	90	5	2×10^{-1}	55	2	18	1×10^{-2}
6×10^5	62	1×10^6	80	5	3×10^{-1}	80	1	24	7×10^{-3}

NOTE.—The number ratio of helium to hydrogen used in all the models is 7×10^{-3} ; all other abundance ratios were assumed equal to their solar values. The radius was chosen so that the energy emitted in Mg II $\lambda 2798$ was equal to its observed value. Calculated strengths of the lines are given in angstroms of equivalent width.

estimated for us an upper limit on the actual equivalent width of [O III] $\lambda 5007$. His upper limit of 15 \AA places a severe requirement on the density (cf. § VIII for a brief discussion of the possibility of photo-ionization for the metastable ¹D state). In Table 4 we give the calculated equivalent widths of the emission lines of major interest obtained from models with total densities in the range ($2.5 \times 10^5 \text{ cm}^{-3}$)–($2 \times 10^7 \text{ cm}^{-3}$). Two different filling factors, $\epsilon = 10^{-3}$ and $\epsilon = 10^{-4}$, were used.

¹ We have tried several schemes, all unsuccessful, in an attempt to avoid such a low helium abundance. One obvious scheme involved a model in which the photon flux was cut off exponentially at 45 eV, a value that lies between the ionization potential of Ne II (41 eV) and that of He II (54 eV). This model does predict, even for a solar helium-to-hydrogen ratio, an unobservably small line emission in He I and He II. However, such a model is unacceptable because it predicts huge equivalent widths for [O III] $\lambda 5007$ and [Ne III] $\lambda 3869$ (the predicted equivalent width for $\lambda 5007$ was 775 \AA , and for $\lambda 3869$ it was 115 \AA). The line at $\lambda 5007$ is very strong in this model because the ionization potentials of He II and O III are practically the same and thus almost all of the oxygen is in the form of O III.

A number of conclusions follow from a comparison of the calculated equivalent widths given in Table 4 with the observed widths given in the last column of Table 2. A density greater than or of the order of $1 \times 10^7 \text{ cm}^{-3}$ is required to prevent the calculated strength of [O III] $\lambda 5007$ from appreciably exceeding the observational upper limit. The strength of the He II line at $\lambda 4686$, which is due to recombination from the predominant ionization stage He III, is almost independent of density. This result reinforces the statements made in the previous subsection regarding the helium abundance in 3C 273. The calculated strength of [Ne III] $\lambda 3869$ is in rough agreement in all cases with the value observed by Schmidt (1968) (cf. Table 2). The calculated strengths of the neutral lines of He I, O I, Ne I, and Mg I are, in all cases, unobservably small. The fact that [Ne V] $\lambda 3426$ is not observed in 3C 273 could imply a large density ($\gtrsim 5 \times 10^7 \text{ cm}^{-3}$), but could also be caused by de-excitation (cf. § VIII). There is no strong reason, on the basis of the calculated line strengths, to prefer either $\epsilon = 10^{-3}$ or $\epsilon = 10^{-4}$. The parameters that seem to characterize best the emission-line region under our assumptions are a radius $R \sim 3\text{--}5 \text{ pc}$, a total density $\sim 1\text{--}5 \times 10^7 \text{ cm}^{-3}$, and a total mass $\sim 1 \times 10^5 M_{\odot}$.

d) Fe II Emission Lines

The calculated strengths of the Fe II lines identified by Wampler and Oke (1967) are in approximate agreement, in our models, with the measured intensities. We have estimated the energy in these lines by using the physical mechanism, but not the mathematical relations, suggested by Wampler and Oke (1967). They suggested that the physical mechanism for production of the line was photo-excitation from the ground states of Fe II to a set of excited states at approximately 5 eV. Occasionally one of the photo-excited levels decays to the metastable levels at approximately 2 eV, a process that gives rise to the observed diffuse emission in the bands at $\lambda\lambda 4450\text{--}4650$ and $\lambda\lambda 5100\text{--}5400$. Wampler and Oke used a set of equations to calculate the energy emitted in the lines of Fe II which, among other things, does not conserve energy. The energy that they calculate for the Fe II lines goes to infinity as the number of scatterings goes to infinity. The actual intensity in the Fe II lines is, of course, bounded by the energy that can be removed from the continuum source.

The basic idea underlying our calculation of the strength of the Fe II lines is energy conservation. Let the optical depth near the Fe II resonance absorption lines be denoted by:

$$\tau(\nu) = \tau_0 x^2 \exp(-x^2), \quad (13a)$$

where

$$x \equiv (\nu - \nu_{12})/\Delta. \quad (13b)$$

The quantity Δ can be estimated from Figure 2 of the paper by Wampler and Oke and is of the order of $5 \times 10^{12} \text{ cycles sec}^{-1}$. Since the optical depth at resonance, τ_0 , is large ($\sim 10^3$ in our models), photons with frequencies near a resonance absorption frequency will be scattered many times. At each scattering the photon has a chance $A_{2m}/A_{21} \sim 3 \times 10^{-4}$ of disappearing from the beam. Here A_{2m} is the average rate of photon decay from the excited states at approximately 5 eV to the metastable states at approximately 2 eV, and A_{21} is the average decay rate from the excited states back to the ground state. Each loss of a resonance photon is accompanied by the appearance of one of the observed photons that are emitted in transitions from states 2 to the metastable states m . According to the calculations of Bahcall (1967), a photon will usually make a transition to a metastable state if $\tau(\nu) (A_{2m}/A_{21})^{1/2}$ is greater than unity. We therefore define a critical frequency ν_{cr} by the relation

$$\tau(\nu_{\text{cr}}) (A_{2m}/A_{21})^{1/2} = 1. \quad (14)$$

Note that ν_{cr} depends only weakly on τ_0 , essentially logarithmically. This weak dependence on τ_0 enables us to make a fair calculation of the emitted energy, even with a

crude model. The basic relation we use for calculating the energy emitted in the Fe II lines is

$$E_{\text{Fe II}} = \int_{\nu_{\text{res}}^-}^{\nu_{\text{res}}^+} \frac{|\nu_{\text{critical}} - \nu_{\text{res}}|}{|\nu_{\text{critical}} - \nu_{\text{res}}|} F_0 d\nu, \quad (15a)$$

$$\approx 2F_0 |\nu_{\text{critical}} - \nu_{\text{res}}|. \quad (15b)$$

Here F_0 is the energy emitted by the continuum source per cycle per second in the frequency range around $\nu_{\text{resonance}}$ and is (cf. eq. [1]) $\sim 8 \times 10^{30}$ ergs sec^{-1} (cps) $^{-1}$. From our models we estimate that, for densities in the range of 10^7 cm^{-3} ,

$$\int \frac{N(\text{Fe II})}{N(\text{Fe})} \frac{dr}{(1 \text{ pc})^3} \sim 2 \text{ to } 3 \times 10^2. \quad (16)$$

Combining equations (13)–(16), we obtain

$$E_{\text{Fe II}} \approx 6 \times 10^{43} \text{ ergs sec}^{-1} \quad (17)$$

if the iron abundance is the same in 3C 273 as in the Sun. The calculated value of $E_{\text{Fe II}}$ is of the same order of magnitude as the observed value (Wampler and Oke 1967).

e) Na I

There is one outstanding exception to the semiquantitative agreement between our calculated line strengths and those measured and identified by the several observers. Wampler and Oke (1967) identified a line with a rest wavelength near 5890 Å with the D-lines of Na I. The D-lines have very small calculated strengths in all our models, since Na I atoms are ionized by the numerous photons with energies greater than 5.1 eV ($\lambda_0 < 2400$ Å). If our models are assumed to be basically correct, then one of three alternatives would seem to be required: (1) there are small, shielded H I regions within the large emission-line cloud, (2) the identification of an observed emission line with Na I is invalid, or (3) the Na I lines arise in a region far from the central source and emission-line cloud.

VII. PARAMETER VARIATIONS

We have investigated the influence on the predicted line strengths of the assumed parameters, the spectral index α and the absolute strength F_0 , that characterize the ionizing continuum spectrum. The predicted line strengths are proportional to the dimensionless integrals $I_{A,i}$, defined in § III. We illustrate in Table 5 the dependence of these integrals on the spectral index. The calculations summarized in Table 5 were carried out for two different values of the spectral index, $\alpha = 0.2$ and $\alpha = 1.2$; the calculations described in § V were performed assuming $\alpha = 0.7$. In all cases the radius of the nebula was fixed by requiring that the predicted line strength for the Mg II doublet agree with the observed line strength. Note that the highest and lowest stages of ionization are strongly influenced by the spectral index. The uncertainty in the predicted line strengths that is due to the uncertainty in the photo-ionization cross-sections is examined in the Appendix. This additional uncertainty is not large for He II, but could be as much as a factor of 3 for Fe II. The change in spectral index from 0.2 to 1.2 changes by a large factor the number of high-frequency photons that produce the highest stages of ionization. The lowest stages of ionization are populated only at the extreme outer edge of the nebula, and a small change in the nebular radius can produce large changes in the integrals $I_{A,i}$ for low stages of ionization. The influence of changes in α is not uniform for all elements. Hence the adjustment of the radius required to produce the correct Mg II emission can introduce large changes in the predicted line strengths for the low stages of

ionization of other elements. The intermediate stages of ionization, such as O III–O VII, maintain relative stability under changes in the spectral index.

The dependence of the strengths of the He II and Fe II lines on α and F_0 is of considerable interest. We found that the predicted He II $\lambda 4686$ line strength is uncertain by a factor of 2, and the Fe II line strengths by a factor of 3, if α is allowed to vary in the range 0.2–1.2 and F_0 in the range 4 to 16×10^{30} ergs sec $^{-1}$ (cps) $^{-1}$.

A change in the assumed value of ϵ from 10^{-3} to 10^{-4} did not affect the relative abundances of any of the observed lines (cf. Table 4) by as much as a factor of 2. However, this variation in ϵ did cause the calculated radius to increase from a typical value of 14 pc for $\epsilon = 10^{-3}$ to 29 pc for $\epsilon = 10^{-4}$. Moreover, the calculated high stages of ionization, which give rise to the predicted coronal lines, were decreased by a factor of the order of 10.

VIII. NECESSARY IMPROVEMENTS

We have made a number of approximations in deriving the models described in previous sections. We indicate here those approximations that are most obviously and urgently in need of improvement (see Tarter 1967 for some possible ways of proceeding). We have investigated whether or not our calculated ionization distribution is consistent with our assumption (cf. eq. [5]) that the main contribution to the opacity, at all frequencies and at all positions in the nebula, comes from hydrogen and helium. We find that our approximation is valid in the outer regions of the nebula where the low stages of ionization dominate. In the inner regions of the nebula, hydrogen and helium are almost completely ionized, and their opacity is consequently small. In this region, however, the contribution from ions of other elements such as C, O, Ne, and Mg is appreciable at high frequencies and should be taken into account in improved models. Our predictions of line strengths from highly ionized atoms are uncertain because (among other things) of our neglect of the opacity of the heavier elements. Our assumption (eq. [3]) that the secondary continuum emission from the large gas cloud is small compared with the continuum emission from the central source is probably not well satisfied, for all positions in the nebula, at wavelengths much shorter than 912 Å. We have also represented the intimate coupling between the radiation field and the kinetic energies of the particles in the crudest possible fashion, namely, by a kinetic temperature that is constant in time and space. We have made a similar oversimplification concerning the total particle density by assuming that it is independent of distance from the central source. We have also neglected (except for the Fe II lines) the contribution of photo-excitation to the emission-line strengths. Photo-excitation is probably significant for many lines, but we do not yet know in a general way the kinds of lines, or the conditions, for which it will be most important. We have not included explicitly photo-excitations out of metastable states. Such processes could in principle decrease greatly the emitted intensities of lines from metastable states, for example, [O II] $\lambda 3727$, [O III] $\lambda 5007$, and [Ne III] $\lambda 3869$ (cf. Pfeiderer and Grewing 1967; Burgess 1967). However, in our models these ions occur only at the outer edge of the emission-line region, and in this area the opacity to photons of the required wavelengths, $\lambda \sim 700\text{--}300$ Å, is so large that the available photon flux is too small to be of importance. The most likely exception to this general statement regarding ions with forbidden-line transitions is [Ne V] $\lambda 3869$, which can exist in regions of somewhat lower opacity. Moreover, there are strong transitions at approximately 150 Å capable of photo-de-exciting the 1D state that gives rise to $\lambda 3869$. The opacity at 150 Å actually is sufficiently small in some of our models to permit the photo-de-excitation of Ne V to occur, but this fact is only suggestive, since we have not included, for example, the opacity of the heavier elements. Many of our models are optically thick to free-free absorption in the wavelength range of several centimeters and longer. If one believes that the varying radio emission comes from the same position as the optical continuum, then the models should be made thin also for radio waves. This could be

TABLE 5
 $I_{A,i}$ FOR TWO VALUES OF α , THE INDEX OF THE CONTINUUM SPECTRUM

ION	STAGE OF IONIZATION											
	I	II	III	IV	V	VI	VII	VIII	IX	X	XI	XII
	$\alpha = 0.2$											
O . . .	7.5×10^{-1}	2.8×10^2	2.6×10^3	6.5×10^3	1.7×10^3	4.2×10^3	9.8×10^3	1.1×10^4	1.1×10^3	5.6×10^3	2.2×10^2	...
Ne . . .	5.3×10^{-2}	1.3×10^1	2.0×10^2	1.1×10^3	2.7×10^3	2.3×10^3	3.4×10^3	8.5×10^3	1.3×10^4	1.1×10^4	7.5×10^3	...
Mg . . .	2.0×10^{-2}	6.8×10^1	4.8×10^1	4.3×10^2	1.1×10^3	1.7×10^3	3.1×10^3	4.9×10^3	5.3×10^3	1.1×10^4	1.6×10^3	...
	$\alpha = 1.2$											
O . . .	2.0×10^{-2}	2.5×10^1	6.4×10^2	2.4×10^3	2.2×10^3	8.0×10^3	8.8×10^3	3.9×10^2	4.2	4.0×10^1	4.6×10^{-1}	...
Ne . . .	4.4×10^{-3}	2.1	1.0×10^2	8.0×10^2	2.8×10^3	4.5×10^3	6.8×10^3	5.7×10^3	1.7×10^3	5.5×10^2	1.2×10^2	...
Mg . . .	1.6×10^{-2}	6.5×10^1	5.0×10^1	6.3×10^2	2.2×10^3	5.8×10^3	7.8×10^3	4.5×10^3	1.2×10^3	3.6		

achieved by requiring that $\epsilon < 10^{-4}$ or by having some essentially empty lanes in the emission-line region (Rees 1968). We have ignored all dynamical effects and, in particular, have not considered the likely possibility (Bahcall 1967) that the emission-line nebula is expanding.

IX. CONCLUSIONS

We summarize here some of the more obvious and important inferences that follow from the calculations described in the previous sections. The ionization equilibrium in the presence of a strong, relatively flat photon flux is different from that in planetary nebulae or in the various theoretical models previously proposed for the emission-line regions of quasi-stellar sources. The variety of ionization stages present in our models is similar to that observed in the nuclei of Seyfert galaxies and may arise from the same mechanism, namely, photo-ionization by a relatively flat spectrum. In particular, we find that high stages of ionization dominate over most of the volume of the nebula; the lower stages of ionization are populated only at the outer edges of the emission-line nebula. In addition to the normally observed emission-lines from low stages of ionization, our models predict the existence of coronal lines in the far infrared. The actual strengths of the predicted coronal lines are, however, extremely sensitive to various parameters and hence are poorly determined in our models. We have obtained semi-quantitative agreement with the strengths of the lines actually observed by calculating the ionization equilibrium in the presence of an extrapolated form of the observed continuum spectrum. The quantities characterizing the emission-line nebula in our models are a radius $R \sim 5$ pc, a total density $N \sim 10^7$ cm $^{-3}$, a fraction of the total volume that is occupied $\epsilon \approx 10^{-3}$ – 10^{-4} , and a total mass of the order of $10^5 M_{\odot}$. The agreement with observation was obtained by using solar elemental abundances except for helium. Our results suggest that the fractional abundances of hydrogen and magnesium are roughly equal to their solar values and that the abundances of oxygen and neon are not much larger than their solar values. The He abundance that gives the best fit to the observed line strengths is about a factor of 10 below the solar helium abundance. Our calculation of the strength of the Fe II lines (cf. § VI*d*) suggests that the fractional abundance of Fe is not too different from the solar iron abundance.

We are grateful to J. B. Oke for valuable conversations and for communicating to us his estimated upper limits for equivalent widths of unobserved lines. It is a pleasure to thank J. L. Greenstein and M. Schmidt for helpful comments on this manuscript and M. Rees for stimulating discussions.

APPENDIX

CROSS-SECTIONS FOR PHOTO-IONIZATION

For the photo-ionization cross-section of H I and He II we used the formula

$$a_{\nu} = a_0(\nu_0/\nu)^3, \quad (\text{A1})$$

where a_0 is the cross-section at the spectral head and ν_0 is the corresponding frequency. The value of a_0 is 6.3×10^{-18} cm 2 for H I and 1.8×10^{-18} for He II. The cross-section for He I was taken from the work of Huang (1948); we used the dipole formula.

Seaton (1958) fitted the cross-sections for ions with configurations $2p^q$ to the polynomial

$$a_{\nu} = 10^{-18} CB \left[a \left(\frac{\nu}{\nu_0} \right)^{-s} + (1 - a) \left(\frac{\nu}{\nu_0} \right)^{-(s+1)} \right]_{\text{cm}^2}. \quad (\text{A2})$$

Seaton gives the constants C , B , a , and s for Ne I-V, Mg III-V, O I-IV, N I-III, C I-II, Na II-V, and Si V.

For the higher stages of ionization of these elements we used the procedure of Williams (1967). He assumed the form

$$a_\nu = B \left(\frac{\nu_0}{\nu} \right)^2, \quad (\text{A3})$$

where B is the value of the cross-section at the spectral head. In order to determine the value of B , he assumed that, for all the ions in the isoelectronic sequence, the absorption cross-section at the spectral head satisfies the relation

$$B = \frac{k}{z + 1}, \quad (\text{A4})$$

where k is the cross-section of the least ionized member of the sequence.

For the cross-section of Mg I, we used the experimental results and extrapolations of Ditchburn and Marr (1953). We extrapolated the theoretical work of Bierman and Lübeck (1949) to obtain a cross-section for Mg II. We also included in our investigations the elements Ar, Si,

TABLE A1
VALUES OF B FROM EQUATION (A3) FOR Si, Ar, AND Fe
(units 10^{-18} cm²)

ION	STAGE OF IONIZATION												
	I	II	III	IV	V	VI	VII	VIII	IX	X	XI	XII	XIII
Si	1 1	4 8	4 5	1 7	3 2	1 0	0 4	1 1	1 2	1 9	0 74
Ar.	35 0	10 0	2 0	4 0	0 8	0 6	0 2	0 03	0 5	0 6	0 24	0 7	0.8
Fe .	1 2	0 24	5 2	3 2	2 5	1 5	0 1	0 01	4 0	2 0	0 6	1 0	0.2

and Fe. Unfortunately, very little theoretical and experimental information is available for the cross-sections of these heavy elements. A summary of the available information can be found in Ditchburn and Öpik (1962). For the cases not discussed by Ditchburn *et al.*, we used rough extrapolations and guesses. We adopted for all these cases an expression of the form of equation (A3). Table A1 contains our estimates for the values of B for Si, Ar, and Fe.

We also examined the sensitivity of our predicted line strengths to changes in the photo-ionization parameters. We calculated, for example, the eleven integrals $I_{\text{Si},i}$ for five different sets of photo-ionization parameters. The first set, A, was the standard set (cf. Table A1) used in our model calculations. The other four sets differed from A in that the cross-section parameters for one ionization stage (per set) were altered. For set B, $B(\text{stage VIII}) = 0.1 B_{\text{standard}}(\text{stage VIII})$; for set C, $B(\text{stage I}) = 7 \times B_{\text{standard}}(\text{stage I})$; for set D, $a^s \propto (\nu/\nu_0)^{-8}$ for stage I; and for set E, $a^s \propto (\nu/\nu_0)^{-8}$ for stage VI. In Table A2 we present the values of the integrals $I_{\text{Si},i}$ obtained using these five sets of photo-ionization parameters. The greatest difference between the integrals calculated for the standard and the altered sets of photo-ionization parameters occurred either in the stage in which the alteration was made or in an adjacent stage. Note that the sensitivity of the integrals $I_{\text{Si},i}$, and therefore the emission-line strengths, to the changes made is not very great.

For the lighter elements H, He, C, N, O, Ne, and Mg we have used fairly accurate cross-sections. Since the sensitivity of the predicted line strengths to changes in the photo-ionization cross-sections is not very great, we conclude that for these lighter elements our ionization calcu-

TABLE A2
 THE INTEGRALS I_A ,¹ FOR THE FIVE DIFFERENT SETS OF PARAMETERS DESCRIBED IN THE APPENDIX

SET No.	STAGE OF IONIZATION											
	I	II	III	IV	V	VI	VII	VIII	IX	X	XI	XII
A...	3.5×10^{-2}	1.9×10^2	4.4×10^2	9.6×10^2	8.8×10^2	3.8×10^3	5.8×10^3	2.8×10^3	2.8×10^3	2.6×10^3	3.3×10^3	1.7×10^3
B...	3.5×10^{-2}	1.9×10^2	4.5×10^2	9.7×10^2	9.2×10^2	4.5×10^3	8.2×10^3	4.9×10^3	5.9×10^3	7.5×10^3	1.4×10^3	1.1×10^3
C...	6.3×10^{-3}	3.4×10^2	7.2×10^2	1.3×10^3	8.3×10^2	3.5×10^3	5.3×10^3	2.6×10^3	2.7×10^3	2.5×10^3	3.3×10^3	1.7×10^3
D...	6.0×10^{-2}	1.8×10^2	4.4×10^2	9.6×10^2	8.8×10^2	3.8×10^3	3.8×10^3	2.8×10^3	2.8×10^3	2.6×10^3	3.3×10^3	1.7×10^3
E...	4.4×10^{-2}	2.4×10^2	5.8×10^2	1.3×10^3	1.3×10^3	6.8×10^3	3.2×10^3	1.8×10^3	2.1×10^3	2.1×10^3	3.0×10^3	1.6×10^3

lations are not appreciably in error due to uncertainties in the photon cross-sections. The uncertainty in the cross-sections is large for the heavier elements, like Ar, Si, and Fe. However, the lack of high sensitivity of the calculated ionization conditions suggests that our results should be at least semiquantitatively correct.

REFERENCES

- Allen, C. W. 1963, *Astrophysical Quantities* (2d ed.; London: Athlone Press).
- Bahcall, J. N. 1967, *Ap. J.*, **145**, 684.
- Bahcall, J. N., Bahcall, N. A., and Shaviv, G. 1968, *Phys. Rev. Letters*, **20**, 1209.
- Bahcall, J. N., and Wolf, R. 1968, *Ap. J.*, **152**, 701.
- Bierman, L., and Lübeck, K. 1949, *Zs. f. Phys.*, **26**, 43.
- Burbidge, G. R., Burbidge, E. M., Hoyle, F., and Lynds, C. R. 1966, *Nature*, **210**, 774.
- Burgess, D. D. 1967, *Nature*, **216**, 1094.
- Ditchburn, R. W., and Marr, G. V. 1953, *Proc. Phys. Soc.*, **A66**, 655.
- Ditchburn, R. W., and Öpik, U. 1962, *Atomic and Molecular Processes*, ed. D. R. Bates (New York: Academic Press).
- Greenstein, J. L., and Schmidt, M. 1964, *Ap. J.*, **140**, 1.
- Huang, S. 1948, *Ap. J.*, **108**, 354.
- Kurt, V. G. 1963, *Soviet Astr.—AJ*, **6**, 620.
- Oke, J. B. 1965, *Ap. J.*, **141**, 6.
- . 1968 (private communication).
- Oke, J. B., and Sargent, W. L. W. 1968, *Ap. J.*, **151**, 807.
- Osterbrock, D. E. 1963, *Planet. and Space Sci.*, **11**, 621.
- Osterbrock, D. E., and Parker, R. A. 1966, *Ap. J.*, **143**, 268.
- Pfleiderer, J., and Grewing, M. 1967, *Science*, **157**, 544.
- Rees, M. 1968 (private communications).
- Schmidt, M. 1963, *Nature*, **197**, 1040.
- . 1964, paper read at 2d Texas Conf. on Relativistic Astrophysics, Austin, Texas, December 1964 (unpublished).
- . 1965, *Ap. J.*, **141**, 1295.
- . 1968 (private communication).
- Seaton, M. J. 1958, *Rev. Mod. Phys.*, **30**, 979.
- . 1960, *Rept. Prog. Phys.*, **23**, 313.
- . 1964, *Planet. and Space Sci.*, **12**, 55.
- Sharov, A. S., and Efremov, Y. N. 1963, *Informational Bull. Var Stars*, No 23, Com. 27, I.A.U.
- . 1964, *Soviet Astr.—AJ*, **7**, 727.
- Shklovsky, I. S. 1965, *Soviet Astr.—AJ*, **8**, 638.
- Smith, H. J., and Hoffleit, D. 1963, *Nature*, **198**, 650.
- Tarter, C. B. 1967, unpublished Ph.D. thesis, Cornell University.
- Wampler, E. J., and Oke, J. B. 1967, *Ap. J.*, **148**, 695.
- Wiese, W. L., Smith, M. W., and Glennon, B. M. 1966, *Atomic Transition Probabilities*, Vol. 1, N.B.S. 4 (Washington, D.C.: U.S. Government Printing Office).
- Williams, R. E. 1967, *Ap. J.*, **147**, 556.
- Woltjer, L. 1967, paper read at 3d Texas Conf. on Relativistic Astrophysics, New York, January.
- Zirin, H. 1966, *The Solar Atmosphere* (Waltham, Mass : Blaisdell Publishing Co), p 133.

